Neuropharmacology 95 (2015) 503–510

Contents lists available at ScienceDirect

Neuropharmacology

journal homepage: www.elsevier.com/locate/neuropharm

Benzothiazepine CGP37157 and its 2′-isopropyl analogue modulate Ca^{2+} entry through CALHM1

Ana J. Moreno-Ortega [a, b], Francisco J. Martínez-Sanz [a], Rocío Lajarín-Cuesta [a], Cristóbal de los Rios [b, **], María F. Cano-Abad [a, *]

[a] Instituto Teófilo Hernando, Departamento de Farmacología y Terapéutica, Universidad Autónoma de Madrid, C/ Arzobispo Morcillo, 4, 28029, Madrid, Spain

[b] Servicio de Farmacología Clínica, Instituto de Investigación Sanitaria, Hospital Universitario de la Princesa, C/ Diego de León, 62, 28006, Madrid, Spain

ARTICLE INFO

Article history:
Received 3 October 2014
Received in revised form
16 January 2015
Accepted 11 February 2015
Available online 20 April 2015

Keywords:
Benzothiazepines
Calcium homeostasis modulator 1 (CALHM1)
CGP37157
ITH12575
Neurodegenerative diseases

Chemical compounds studied in this article:
CGP37157
PubChem CID: 2688
Dimebolin
PubChem CID: 197033
Carbonyl cyanide-*p*-trifluoromethoxyphenylhydrazone
FCCP
PubChem CID: 3330

ABSTRACT

CALHM1 is a Ca^{2+} channel discovered in 2008, which plays a key role in the neuronal electrical activity, among other functions. However, there are no known efficient blockers able to modulate its Ca^{2+} handling ability. We herein describe that benzothiazepine CGP37157 and its newly synthesized analogue ITH12575 reduced Ca^{2+} influx through CALHM1 at low micromolar concentrations. These results could serve as a starting point for the development of more selective CALHM1 ligands using CGP37157 as a hit compound, which would help to study the physiological role of CALHM1 in the control of $[Ca^{2+}]_{cyt}$ in excitable cells, as well as its implication in CNS diseases.

1. Introduction

Since the discovery of the channel CALHM1 (Ca^{2+} Homeostasis Modulator 1) in 2008 (Dreses-Werringloer et al., 2008), several papers have discussed whether this channel is implicated in the progression of certain CNS (central nervous system) diseases, not only Alzheimer's disease (AD) (Koppel et al., 2011), but also temporal lobe epilepsy (Lv et al., 2011) and Creutzfeldt-Jakob's disease (Calero et al., 2012). Six human CALHM1 homologous have been characterized, with different splicing and expression throughout the organism (Ma et al., 2012). CALHM1 has been proposed to be the pore-forming subunit of a cation channel, which would modulate the extracellular Ca^{2+}-controlled neuronal excitability and the Ca^{2+} homeostasis, in the so-called Ca^{2+} add-back conditions (Ma et al., 2012). CALHM1 is located in plasma membrane and endoplasmic reticulum (ER), where its alteration could lead to Ca^{2+} homeostasis disruption, ER stress, and cell damage (Gallego-Sandin et al., 2011). In summary, it seems that CALHM1 plays an essential role in the neuronal electrical activity by controlling the intracellular Ca^{2+}-derived signal transduction (Dreses-Werringloer et al., 2013). Heterologous expression of human CALHM1 in *Caenorhabditis elegans* has revealed its physiological role in biolocomotion, though its overexpression causes neurodegeneration through a Ca^{2+}-dependent necrotic-like mechanism (Tanis et al.,

* Corresponding author.
** Corresponding author.
E-mail address: maria.cano@uam.es (M.F. Cano-Abad).

http://dx.doi.org/10.1016/j.neuropharm.2015.02.016
0028-3908/

2013). Furthermore, CALHM1 might have peripheral physiological functions, as it is expressed in taste buds and it has been hypothesized that it controls the taste perception (Taruno et al., 2013; Tordoff et al., 2014). From a physiopathological point of view, CALHM1 controls cytosolic Ca^{2+} concentration ($[Ca^{2+}]_{cyt}$) and amyloid beta peptide (Aβ) levels in depolarizing conditions (Dreses-Werringloer et al., 2008). When the polymorphism P86L-CALHM1 (rs2986017) is present, a deregulation of such $[Ca^{2+}]_{cyt}$ and Aβ levels are found (Dreses-Werringloer et al., 2008), generating Aβ accumulation as well as mitochondrial Ca^{2+} ($[Ca^{2+}]_{mit}$) overload (Moreno-Ortega et al., 2010). Despite these findings, there is no agreement in the role played by CALHM1 in AD progression, as some papers describe a lack of correlation between the polymorphism P86L-CALHM1 and the risk of suffering AD (Giedraitis et al., 2010; Inoue et al., 2010; Tao et al., 2014). By contrast, Lambert et al., in an international meta-analysis, established that P86L-CALHM1 is not a genetic factor, but it might modulate the age of AD onset (Lambert et al., 2010). Studies focused on clarifying the role of CALHM1 have to recruit molecular biology techniques (Dreses-Werringloer et al., 2013) due to the lack of drugs capable of regulating its activity. Some metals and metal-organic complexes at high concentrations, e.g. Co^{2+} (100 μM), Zn^{2+} (20 μM), Ni^{2+} (10 μM), Gd^{3+} (100 μM), 2-aminoethoxydiphenyl borate (2-APB; 1 mM) or ruthenium red (20 μM), block Ca^{2+} entry through CALHM1 (Dreses-Werringloer et al., 2013; Ma et al., 2012).

In this paper, we present the first organic compound capable to block the Ca^{2+} uptake through CALHM1 at low micromolar concentrations, the benzothiazepine CGP37157 (7-chloro-5-(2-chlorophenyl)-3,5-dihydro-4,1-benzothiazepin-2-(1*H*)-one, Fig. 1), which has been widely used as a mitochondrial Na^{+}/Ca^{2+} exchanger (mNCX) blocker (Chiesi et al., 1988; Pei et al., 2003). This compound and some of its analogues have shown a neuroprotective profile in several in vitro models of AD and stroke (Gonzalez-Lafuente et al., 2012; Nicolau et al., 2009, 2010). In addition, we herein prove the CALHM1 blocking activity of one of its derivatives, synthesized in our research group, ITH12575 (7-chloro-5-(2-isopropylphenyl)-3,5-dihydro-4,1-benzothiazepin-2-(1*H*)-one, Fig. 1), which has shown the most interesting neuroprotective properties (unpublished results). Our results will help to clarify the actual contribution of CALHM1 to physiological/pathological events implicating cell Ca^{2+} dynamics.

2. Material and methods

2.1. Reagents

Coelenterazine was purchased from Biotium (Hayward, USA). Dimebolin was purchased from Biotrend Chemikalien GmbH (Cologne, Germany). Metafectene was purchased from Biontex (Martinsried/Planegg, Germany). Digitonin and $CoCl_2$, and other general chemicals were purchased from Sigma (Madrid, Spain). CGP37157 was purchased from Tocris (Madrid, Spain).

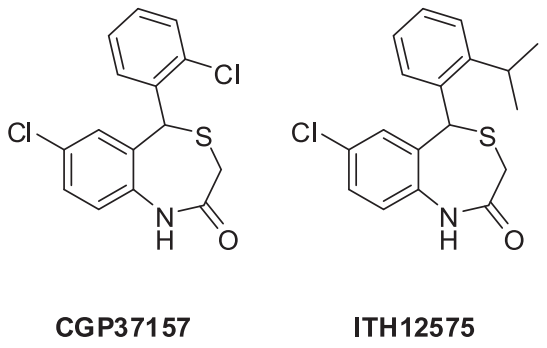

Fig. 1. Chemical structures of the benzothiazepines CGP37157 and ITH12575.

2.2. HeLa cells source, culture, and transfection

HeLa cells were grown in plastic flasks in DMEM supplemented with 10% fetal bovine serum, 2 mM glutamine, 25 U/mL penicillin and 25 μg/mL streptomycin (all products were obtained from Lonza (Basel, Switzerland)). The experiments were performed with cells seeded on 13-mm diameter coverlips, in 24-well plates and grown to 60–70% confluence after 24 h in the incubator at 37 °C and 5% CO_2. Transient co-transfections with the genetically encoded photoprotein aequorin, targeted to the cytosol (cyt_AEQ) and CALHM1 or P86L-CALHM1, in a ratio 1:1, were achieved by using Metafectene (Biontex, Martinsried/Planegg, Germany) (Diaz-Prieto et al., 2008). Experiments to measure $[Ca^{2+}]_{cyt}$ changes were performed 36–48 h after transfection. The two recombinant proteins were expressed in the same subset of cells.

2.3. Measurements of $[Ca^{2+}]_{cyt}$ with aequorin

HeLa cells expressing cyt_AEQ were reconstituted by incubating cells 1.5 h with 5 μM wild type coelenterazine before the experiment. The cell monolayer was continuously superfused with Krebs–HEPES buffer (KHB) of the following composition (mM): 125 NaCl, 5 KCl, 1 Na_3PO_4, 1 $MgSO_4$, 5.5 glucose, 20 HEPES, with pH 7.4 at room temperature (24 ± 2 °C); the zero Ca^{2+} solution contained 0.5 mM EGTA (ethylene glycol tetraacetic acid). To induce Ca^{2+} entry, KHB deprived of Ca^{2+} with EGTA was changed by another solution containing 1 mM $CaCl_2$, as specified in figure legends. Light emission was measured in a purposed-built luminometer and calibrated in terms of $[Ca^{2+}]$. At the end of the experiment, cells were lysed by superfusing them with KHB containing 10 mM $CaCl_2$ and 100 μM digitonin, in order to expose cells to excess Ca^{2+} to burn out the aequorin remaining at the end of each experiment.

2.4. Data analysis

Data are presented as means ± SEM. Peak increases of the $[Ca^{2+}]_{cyt}$ elevations and areas under the curve (AUC) were determined by using Origin v. 5.0 (OriginLab Corporation, Northampton, USA). Statistical differences were assessed by ANOVA test followed by Bonferroni's or Newman–Keuls' post hoc analysis. Statistical differences were taken as significant when $p \leq 0.05$. All statistical analyses were performed using a Prism software (GraphPad) version 5.0 for Mac (OS X).

2.5. Chemical synthesis of ITH12575

Reactions were monitored by thin layer chromatography using precoated silica gel plates. Detection was made with light UV at 254 nm. Pre-charged silica gel columns were used in a Biotage chromatography station (230–400 mesh). Melting points were determined in a Stuart apparatus (SMP-10) and are not corrected. MS spectra were obtained in a QSTAR de ABSciex apparatus. ^{1}H and ^{13}C NMR spectra were carried out with a Bruker AVANCE 300 MHz. Elemental analyses were used as a purity criteria and performed on a LECO CHNS-932 station. Compounds described had a purity of 95% or more. For the determination of absolute configuration, single crystal X-ray diffractions have been performed, using a Bruker Kappa Apex II apparatus with a Mo source and graphite monochromater.

2.5.1. Synthesis of 4-chloro-N-tert-butoxycarbonylaniline (**1**)

To a solution of 4-chloroaniline (1 g, 7.84 mmol) in dry tetrahydrofurane (THF) (65 mL), tert-butyl dicarbonate (1.88 g, 8.62 mmol) and triethylamine (872 mg, 1.2 mL, 8.62 mmol) were added. The reaction mixture was stirred at room temperature for 48 h, after then solvent was evaporated and ethyl acetate (300 mL) was added. The solution was washed with saturated NH_4Cl (2 × 100 mL) and water (2 × 100 mL). The organic layer was dried over $MgSO_4$, filtered and evaporated, obtaining a solid white showing spectral data according to **1** (yield 99%) (Roosen et al., 2012). It was used with no further purification.

2.5.2. Synthesis of o-isopropylbenzaldehyde (**2**)

To a solution of 1-bromo-2-isopropylbenzene (388 mg, 298 μL, 1.95 mmol) in dry THF, n-butyllithium (2.5 M in hexanes, 858 μL, 2.14 mmol) was added dropwise at −78 °C. After 20 min at −78 °C, dimethylformamide (157 mg, 166 μL, 2.14 mmol) was added and the reaction mixture was stirred at −78 °C for 20 min and allowed to heat up to −10 °C and stirred for 3 h more. Reaction was stopped by adding water (2.5 mL) and extracted with diethyl ether (3 × 100 mL). Combined organic layers were dried over anhydrous $MgSO_4$, filtered, and evaporated, affording **2** with quantitative yield as a colorless oil (277 mg) showing spectral data according to its structure (Ewing, 1974). It was used with no further purification.

2.5.3. Synthesis of 4-chloro-2-[hydroxy(2-isopropylphenyl)methyl]-N-tert-butoxycarbonylaniline (**3**)

To a solution of **1** (496 mg, 2.18 mmol) in dry THF (15 mL), tert-butyllithium (1.7 M, 3.49 mL, 5.93 mmol) was added dropwise at −78 °C and the reaction was stirred at this temperature for 15 min, then it was stirred for 2 h at −20 °C. After this time, reaction was cooled down to −78 °C and **2** (358 mg, 2.55 mmol) in dry THF (5 mL) was added dropwise and the reaction was allowed to stir 2 h at this temperature. Reaction was terminated by addition of water (15 mL) and once it reached room temperature, it was extracted with diethyl ether (3 × 30 mL) and the

combined organic layer washed with brine (3 × 50 mL), dried over anhydrous $MgSO_4$, filtered and evaporated, to obtain a yellow oil that was purified by flash chromatography (ethyl acetate:hexanes, 1:18), affording compound **3** with a 67% yield. ^{1}H NMR (300 MHz, $CDCl_3$) δ 7.85 (d, 1H, J = 8.6 Hz, H6), 7.42 (s, 1H, NH), 7.38–7.10 (m, 6H, H_{Ar}), 6.90 (d, 1H, J = 2.0 Hz, H3), 6.10 (s, 1H, CH), 3.00 [heptet, J = 7.0 Hz, 1H, $CH(CH_3)_3$], 2.45 (bs, 1H, OH), 1.41 (s, 9H, CH_3), 1.23 (d, J = 7.0 Hz, 3H, CH_3), 1.18 (d, 3H, J = 7.0 Hz, CH_3).

2.5.4. Synthesis of 7-chloro-5-(2′-isopropylphenyl)-3,5-dihydro-4,1-benzothiazepin-2-(1H)-one (*ITH12575*)

To a solution of methyl thioglycollate (172 mg, 148 μL, 1.62 mmol) in trifluoroacetic acid (431 mg, 289 μL, 3.78 mmol) compound **3** (100 mg, 0.27 mmol) was added. The reaction mixture was stirred at 85 °C for 24 h and it was dissolved in CH_2Cl_2 (30 mL). The crude was washed with brine (30 mL), 1N $NaOH_{aq}$ (30 mL), and brine (30 mL), dried over Na_2SO_4, filtered, and evaporated, to obtain a brown oil that was purified by flash chromatography (ethyl acetate:hexanes, 1:3), affording compound **4** as a white solid, with a 62% yield. Melting point: 188–190 °C. ^{1}H NMR (300 MHz, $CDCl_3$) δ 8.16 (s, 1H, NH), 7.75 (dd, 1H, J = 8.5, 2.0 Hz, H8), 7.43–7.31 (m, 3H, H_{Ar}), 7.29–7.21 (dd, 1H, H5′), 7.07 (d, J = 8.5, 1H, H9), 6.81 (d, J = 2.0 Hz, 1H, H6), 6.10 (s, 1H, H5), 3.40 and 3.01 (AB, J = 12.3, CH_2), 2.82 [heptet, J = 6.8 Hz, 1H, $CH(CH_3)_3$], 1.22 (d, J = 6.8 Hz, 3H, CH_3), 0.87 (d, J = 6.8 Hz, 3H, CH_3). Anal. ($C_{18}H_{18}ClNOS$) C, H, N, and S similar to the experimentally found data.

2.6. Chiral separation procedure of ITH12575

High Performance Liquid Chromatography with Ultraviolet and Mass detection (HPLC/MS) was used for the development of conditions for the resolution of the racemic mixture of ITH12575, as well as for the determination of the enantiomeric excess (ee) of the two enantiomers isolated by semipreparative chiral HPLC. Chromatographies were performed on CHIRALPAK AD [amylose tris (3,5-dimethylphenyl carbamate)] units. The column dimensions were 100 × 4.6 mm and 250 × 20 mm for analytical and semi-preparative work, respectively. In both units, the enantioselective phase was coated onto silica-gel substrate (10 μm). Experiments were carried out at room temperature. Flow rate was set up at 0.2 and 65 mL/min for analytical and semipreparative work, respectively. Mobile phase consisted of 0.2% IPAm/methanol, for analysis, and CO_2 (A)/methanol-DMEA (0.2% v/v) (B) Isocratic 10% B, for purification. In all cases, the wavelength of UV detection was monitored from 200 to 400 nm although chromatograms were recorded at 220 and 254 nm signals. Mass spectra were recorded using API-APCI ionization (full scan in positive/negative modes simultaneously). Retention time at analytical scale for the two target enantiomers are 1.08 and 1.30 min. Chiral quality control of isomers isolated (**AT1** and **AT2**) by semi-preparative HPLC confirmed ee >98% for the two target compounds. **AT1** (Ret. time = 1.08 min) showed an $[\alpha]_D$ of −411.6 (*c* 0.61, CH_2Cl_2). **AT2** (Ret. time = 1.30 min) showed an $[\alpha]_D$ of +425.9 (*c* 0.69, CH_2Cl_2).

2.7. Single crystal X-Ray diffraction data for (−)-ITH12575 (*AT1*) and (+)-ITH12575 (*AT2*)

Diffraction data were collected on a Bruker Kappa Apex II diffractometer equipped with Mo source and a graphite monochromator. The software package SHELXTL was used for space group determination, structure solution, absorption correction and refinement[1]. The structures were solved by direct methods, completed with difference Fourier syntheses, and refined with anisotropic displacement parameters. In both structures, carbon atoms C17 and C18, from the terminal methyl groups, were found at two alternate positions. A statistical disorder model was made to account for this situation, and the occupation factor refined for a final value of 56% for part A and 44% for part B in **AT1**; and 55% for part A and 45% for part B in **AT2**.

CCDC 1021365 and 1021366 contain the supplementary crystallographic data for compounds **AT1** and **AT2**. These data can be obtained free of charge at www.ccdc.cam.ac.uk/conts/retrieving.html [or from the Cambridge Crystallographic Data Centre, 12, Union Road, Cambridge CB2 1EZ, UK; fax: +44 1223/336-033; e-mail: deposit@ccdc.cam.ac.uk].

3. Results and discussion

3.1. Co^{2+} blocks Ca^{2+} entry through both CALHM1 and P86L-CALHM1 but not in blank-transfected HeLa cells

To study the pharmacological modulation of CALHM1, we used HeLa cells transfected with the genetically encoded photoprotein aequorin targeted to the cytosol (cyt_AEQ), (Moreno-Ortega et al., 2010) achieved with Metafectene (Diaz-Prieto et al., 2008). HeLa cells do not express plasmalemmal Na^+/Ca^{2+} exchanger or voltage-gated Ca^{2+} channels (VGCC). Thus, they are an excellent model for the study of the expression and function of Ca^{2+} channels such as CALHM1. Either wild type CALHM1 or its polymorphism P86L-CALHM1 were transiently co-transfected with aequorins, in a ratio 1:1. Luminescence experiments were performed as previously described (Moreno-Ortega et al., 2010). Cells were first perfused with a 0 Ca^{2+}/EGTA solution for 2 min, after which it was replaced by another solution containing 1 mM Ca^{2+} (no EGTA). HeLa cells transfected with CALHM1 showed an apparent increase in the Ca^{2+} entry when reintroducing the extracellular Ca^{2+}, compared with that found in control cells. Similarly to previous observations by other authors (Dreses-Werringloer et al., 2008), the increases in both maximal peak and the area under the curve (AUC) were blocked by Co^{2+} 100 μM, used as a standard, non-specific Ca^{2+} channels blocker, in 87 and 89%, respectively, (Fig. 2). Regarding to the P86L-CALHM1-transfected cells, they underwent a lower increase in both $[Ca^{2+}]_{cyt}$ peak and AUC, together with a slower rise rate, as reported by our group (Moreno-Ortega et al., 2010) In these cells, Co^{2+} 100 μM completely abolished peak of $[Ca^{2+}]_{cyt}$ and AUC increases (Fig. 2).

3.2. Antihistaminic, and antiamyloidogenic drug dimebolin does not affect Ca^{2+} permeability through CALHM1 or P86L-CALHM1 in HeLa cells

In the search for new chemical entities capable of modulating CALHM1-dependent $[Ca^{2+}]_{cyt}$ homeostasis, we aimed to study neuroprotective drugs of our own chemical library that had been described to block ionic channels, preferentially VGCC, following the hypothesis previously by other authors (Dreses-Werringloer et al., 2008; Ma et al., 2012), who had focused on a huge variety of ionic channels blockers in order to modulate the CALHM1 signal. Among several compounds studied, we present dimebolin as an example, which is a non-selective antihistamine drug with multiple mechanisms of action including L-type VGCC blockade, protection against the Aβ-induced neurotoxicity and the reduction of the mitochondrial swelling induced by toxic insults (Bachurin et al., 2003; Cano-Cuenca et al., 2014; Lermontova et al., 2001). In all the experimental conditions performed, dimebolin 20 μM had no effect on Ca^{2+} signaling, neither on peak nor AUC increases (Fig. 3).

3.3. Neuroprotectant and mitochondrial Na^+/Ca^{2+} exchanger blocker CGP37157 reduces Ca^{2+} permeability through CALHM1 but not through P86L-CALHM1 in HeLa cells at low micromolar concentrations

By contrast, when we tested the mNCX blocker CGP37157, a reduction of the CALHM1-controlled Ca^{2+} permeability was observed (Fig. 4). When applied to HeLa cells transfected with CALHM1 at 0.1 μM, CGP37157 blocked by 57% and 44% the maximal peak of $[Ca^{2+}]_{cyt}$ and the AUC, respectively, induced by the Ca^{2+} reintroduction. Similar blockades in $[Ca^{2+}]_{cyt}$ peak and AUC were found at 0.3 μM (50% and 40%, respectively) and 1 μM (36 and 32%, respectively) (Fig. 4D and E). CGP37157 at 3 μM did not affect the $[Ca^{2+}]_{cyt}$ signal in a significant manner, but when applied at 10 and 30 μM, CGP37157 reduced maximal peak of $[Ca^{2+}]_{cyt}$ by 26% and 39%, respectively, but lacking statistical significance. The weird behavior of CGP37157 could be due to the lack of target selectivity when doses reach higher micromolar levels. HeLa cells transfected with the P86L-CALHM1 presented a different sensitivity to the administration of CGP37157, as no significant reduction of Ca^{2+} signals was observed at any concentration, but even 10 and 30 μM CGP37157 evoked an augmentation in either AUC and maximal peak of $[Ca^{2+}]_{cyt}$, respectively (Fig. 4D and E).

[1] SHELXTL version 6.12, Structure Determination Package, Bruker, Madison, Wisconsin, USA, 2001.

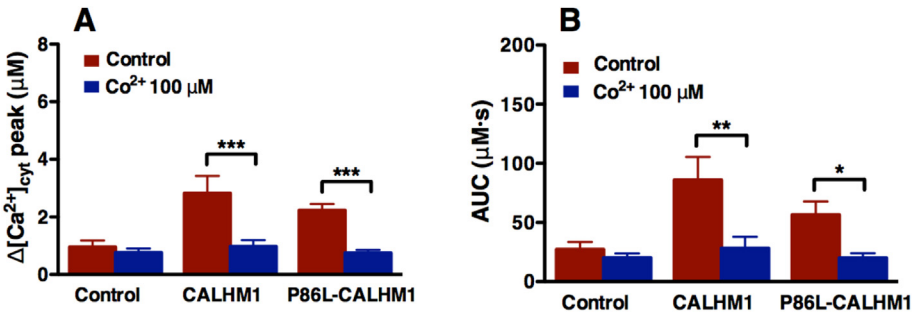

Fig. 2. Effect of Co^{2+} on the CALHM1-controlled Ca^{2+} permeability. Cells were transiently transfected with blank (Control), CALHM1, or P86L-CALHM1. Cells were perfused with Co^{2+} at 100 μM for 2 min before and during the pulse of 1 mM Ca^{2+}. Panel A shows the mean of peak increases of the $[Ca^{2+}]_{cyt}$ elevations and Panel B shows the area under the curve (AUC) of cytosolic Ca^{2+} in HeLa cells. Mean of at least 9 experiments for each transfection protocol, made with cells from 3 different cultures. Data are means ± SEM. $^{*}p < 0.05$, $^{**}p < 0.01$, $^{***}p < 0.001$.

3.4. Reduction of Ca^{2+} permeability through CALHM1 elicited by CGP37157 is independent to its effect on the mitochondrial Ca^{2+} buffering capacity

These results confirm that CGP37157 is the first organic compound modulating Ca^{2+} entry through CALHM1 at very low concentrations. Nevertheless, we wondered whether this regulation is actually due to an indirect effect on the mNCX. To answer this question, we carried out similar experiments in the presence of the ionophore FCCP (carbonyl cyanide-*p*-trifluoromethoxyphenylhydrazone) (Mitchell and Moyle, 1967), thus abolishing the regulatory action on the $[Ca^{2+}]_{cyt}$ performed by mitochondria (Fig. 5).

Fig. 5A, B, and C show an additional transient elevation of $[Ca^{2+}]_{cyt}$ during the 0 Ca^{2+} interval when FCCP 1 μM is administered. This $[Ca^{2+}]_{cyt}$ oscillation is due to the emptying of the stored Ca^{2+} in organelles by the protonophore FCCP. In any case, when Ca^{2+} permeability of CALHM1 is achieved by the reintroduction of extracellular Ca^{2+} 1 mM, plus preincubation with the cocktail of FCCP and CGP37157 1 μM, a similar reduction in $[Ca^{2+}]_{cyt}$ signal was maintained, (expressed as an augmentation of $[Ca^{2+}]_{cyt}$ peak and AUC (Fig. 5D and E, respectively), comparing HeLa cells exposed only to FCCP with cells exposed to FCCP plus CGP37157, expressed as an augmentation of $[Ca^{2+}]_{cyt}$ peak and AUC (Fig. 5D and E, respectively). Again, P86L-CALHM1 polymorphism seems insensitive to CGP37157 in terms of $[Ca^{2+}]_{cyt}$ oscillations. These data suggest that pharmacological actions of CGP37157 were not due to its blockade of mNCX. However, further experiments need to be addressed in order to point out a direct interaction of CGP37157 on CALHM1.

3.5. CGP37157 derivative ITH12575 slightly reduces Ca^{2+} permeability through CALHM1 in an enantiospecific fashion

Additional studies were carried out with the CGP37157 derivative ITH12575 (Fig. 1), synthesized in our laboratory (see Materials and methods), which has shown an improved

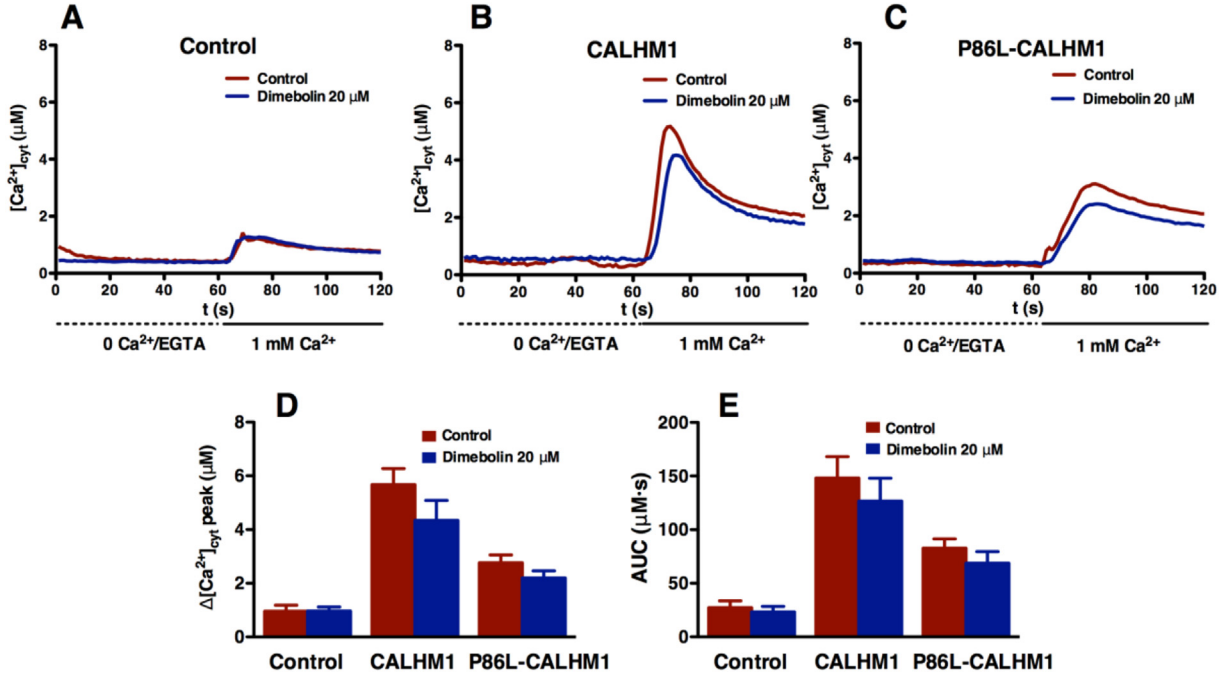

Fig. 3. Effect of dimebolin on the CALHM1-controlled Ca^{2+} permeability. Panels A, B, and C show typical $[Ca^{2+}]_{cyt}$ registers when cells were transiently transfected with blank, CALHM1, or P86L-CALHM1, respectively. Cells were perfused with Dimebolin at 20 μM for 2 min before and during the 1 mM Ca^{2+} pulse. Panel D shows the mean of peak of the $[Ca^{2+}]_{cyt}$ elevations and Panel E shows the area under the curve (AUC) of the Ca^{2+} transients in HeLa cells transfected with blank (Control), CALHM1 or P86L-CALHM1. Mean of at least 9 experiments for each transfection protocol, made with cells from 3 different cultures. Data are means ± SEM. No significant differences were found.

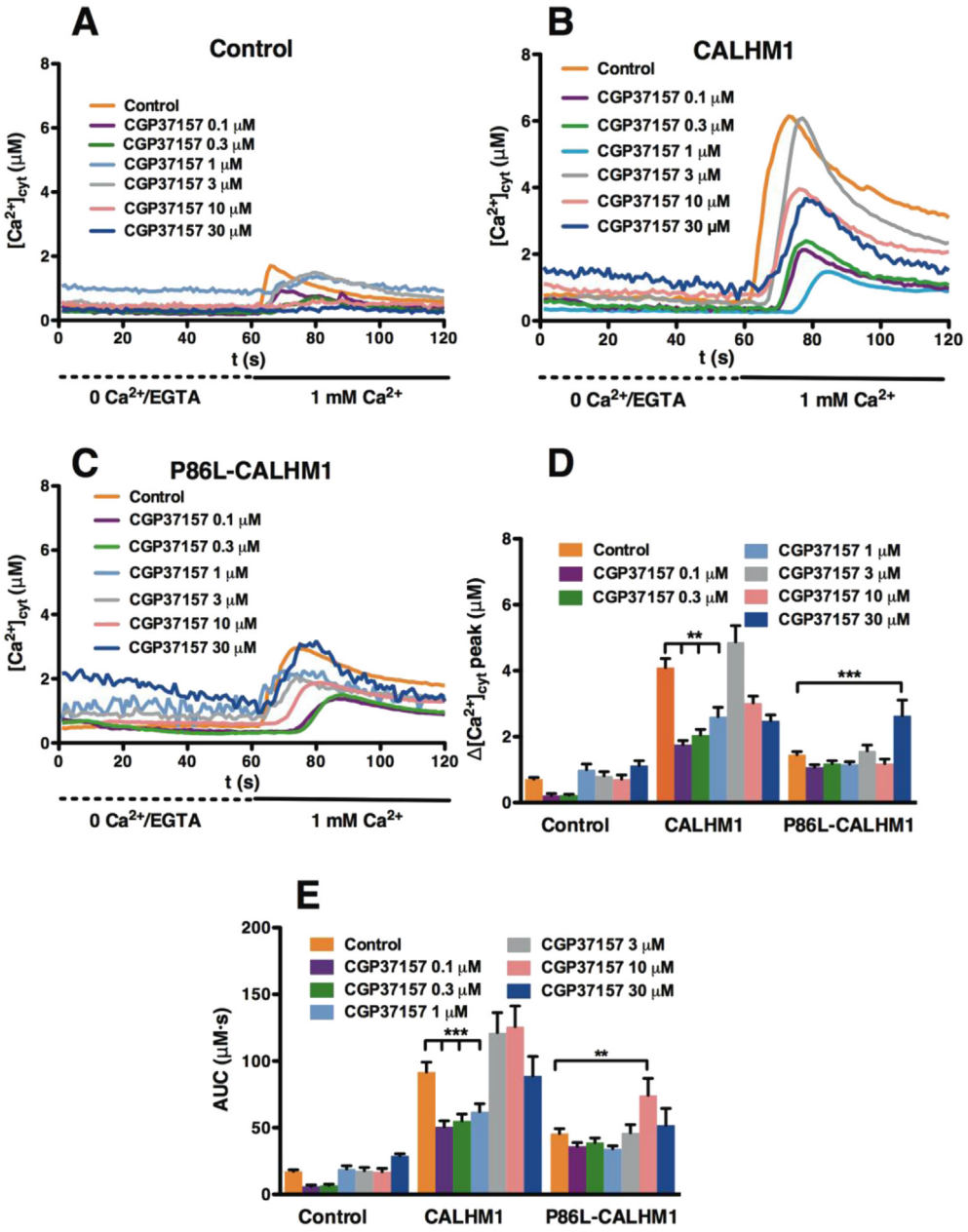

Fig. 4. Intracellular Ca^{2+} responses induced by CALHM1 and P86L-CALHM1. Concentration–response curves of CGP37157. Panels A, B, and C show typical registers of $[Ca^{2+}]_{cyt}$ when cells were transiently transfected with blank, CALHM1, or P86L-CALHM1, respectively. CGP37157, at 0.1–30 μM, was perfused for 2 min before and during the 1 mM Ca^{2+} pulse. Panel D shows the mean of peak increases of the $[Ca^{2+}]_{cyt}$ signal and panel E shows the area under the curve (AUC) of the Ca^{2+} transients in HeLa cells transfected with blank (Control), CALHM1 or P86L-CALHM1. Mean of at least 6 experiments for each transfection protocol, made with cells from 3 or more different cultures. Data are means ± SEM. *$p < 0.05$, **$p < 0.01$, ***$p < 0.001$.

neuroprotective profile (data not shown). ITH12575, at 1 μM, did not block CALHM1 or P86L-CALHM1 permeability. However, considering that it is a racemic compound, a possibility exists that one enantiomer could preferentially interact with CALHM1 or P86L-CALHM1. Thus, after HPLC-conducted chiral separation, we resolved the absolute configuration of both enantiomers by single crystal X-ray diffraction (Supplementary data), reporting that enantiomer with lesser retention time in HPLC (**AT1**, 1.08 min) and *levo* rotatory optical deviation ($[\alpha]_D$ of −411.6 (*c* 0.61, CH_2Cl_2)) corresponded to the (−)-R-enantiomer of ITH12575, whilst the enantiomer with greater retention time in HPLC (**AT2**, 1.30 min) and *dextro* rotatory optical deviation ($[\alpha]_D$ of +425.9 (*c* 0.69, CH_2Cl_2)) corresponded to the (+)-S-enantiomer of ITH12575 (see Reports and 3D, CIF structures in supplementary material). Hence, when testing each enantiomer separately, we observed that (+)-S-ITH12575 blocked both increase of $[Ca^{2+}]_{cyt}$ peak and AUC of Ca^{2+} entry through the wild type CALHM1 by 47 and 46%, respectively. Additional experiments were carried out to evaluate the concentration-dependency of the S-enantiomer of ITH12575. Unfortunately, the other concentrations assayed (0.1 and 10 μM) were ineffective to block CALHM1 (see Supplementary material, Fig. S3). Once more, P86L-CALHM1 was insensitive to the exposure of ITH12575, neither racemic nor optically pure compounds (Fig. 6).

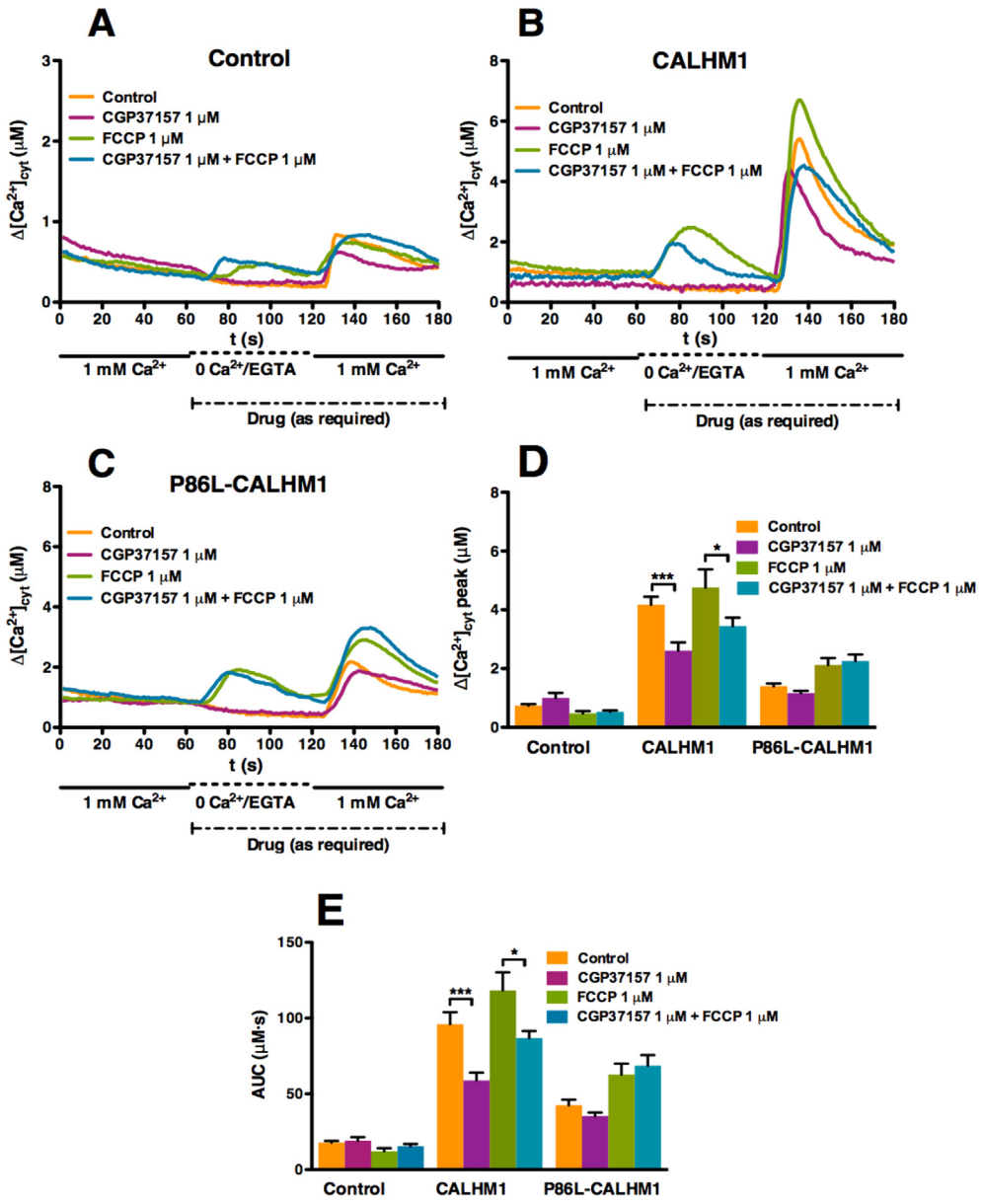

Fig. 5. CALHM1 blockade with CGP37157, upon ablation of mitochondria Ca^{2+} buffering with FCCP. Panels A, B, and C show typical $[Ca^{2+}]_{cyt}$ registers when cells were transiently transfected with blank, CALHM1, or P86L-CALHM1, respectively, in presence of CGP37157 1 μM and/or FCCP 1 μM. Panel D shows the mean of peak of the $[Ca^{2+}]_{cyt}$ elevations and panel E shows the AUC of the Ca^{2+} transients in HeLa cells transfected with blank (Control), CALHM1 or P86L-CALHM1. Mean of at least 9 experiments for each transfection protocol, made with cells from 4 or more different cultures. Data are means ± SEM. $^{*}p < 0.05$, $^{***}p < 0.001$.

4. Conclusions

In summary, we have found an organic compound acting as a CALHM1 channel regulator, the benzothiazepine CGP37157, able to reduce Ca^{2+} entry through CALHM1 at very low concentrations. Previously described blockers, such as Co^{2+}, have to be administered at much higher concentrations. CGP37157 reduced Ca^{2+} influx with no concentration-dependent manner. A possibility exists to ascribe this behavior to additional interactions of CGP37157 with other biological targets expressed in HeLa cells that are also contributing to the cell Ca^{2+} handling and thus modifying the Ca^{2+} uptake via CALHM1. The pharmacological actions of CGP37157 over CALHM1 should be more deeply studied, to explain its lack of concentration-dependent activity. These effects are presumably due to the interaction of CGP37157 with other biological targets, e.g. mNCX or sarco-endoplasmic Ca^{2+} ATPase (SERCA), and the subsecuent Ca^{2+} cell dynamics alteration when administered at higher micromolar concentrations (Ragone et al., 2013). Moreover, though we have discarded that CCGP37157 exerts its modulatory effect on CALHM1 indirectly through mitochondria, further experiments need to be addressed to confirm a direct action on CALHM1. Nevertheless, observing the pharmacological tools available up to date to study CALHM1, this work would represent a significant breakthrough, as CALHM1 functionality can be more finely dissected by applying CGP37157 at 0.3 μM, for instance. This work should serve as a starting point for the development of better CALHM1 ligands, using CGP37157 as a hit compound. The optimization of the pharmacological activity of CGP37157 over CALHM1 will help to get a better comprehension of the role of CALHM1 in the control of $[Ca^{2+}]_{cyt}$ in excitable cells, as well as the implication of its mutated form in the development of CNS like AD.

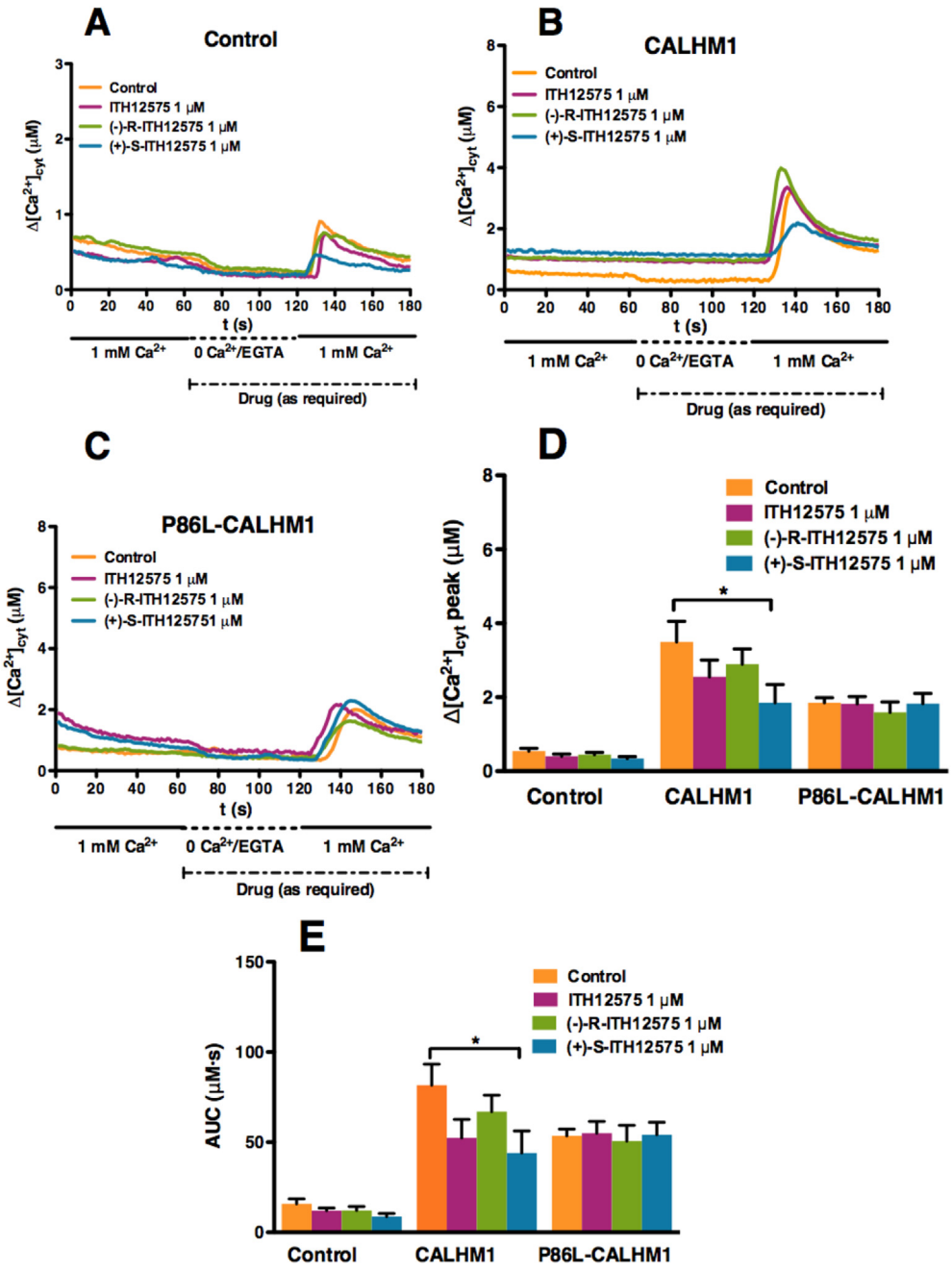

Fig. 6. Effect of ITH12575 and its enantiomers on the CALHM1-induced Ca^{2+} entry. Cells were transiently transfected with blank (A), CALHM1 (B), or P86L-CALHM1 (C), and a Ca^{2+} add-back protocols were carried out in presence of the rac-, S- or R-ITH12575 1 μM. Compounds were perfused at 1 μM for 2 min before and during the 1 mM Ca^{2+} pulse. Panel D shows the mean of peak of the $[Ca^{2+}]_{cyt}$ elevations and panel E shows the AUC of the Ca^{2+} transients in HeLa cells transfected with blank (Control), CALHM1, or P86L-CALHM1. Mean of at least 8 experiments for each transfection protocol, made with cells from 4 or more different cultures. Data are means ± SEM. *$p < 0.05$.

Acknowledgment

We thank the generous gifts of cDNAs for CALHM1 and P86L-CALHM1 to Dr. Philippe Marambaud, Litwin-Zucker Research Center for the study of Alzheimer's disease (N.Y.), and cDNA for cyt_AEQ to Prof. Tullio Pozzan, University of Padova (Italy). This work supported by the following grants: to M.F.C.A.: Consolidación de Grupos UAM-CAM (ref. 1004040047); to C.d.l.R: Proyectos de Investigación en Salud (PI13/00789, IS Carlos III). A.J.M.O. is granted by Ministry of Economy (FPU program, ref. AP2009/0343). R.L.-C. thanks Universidad Autonoma de Madrid for predoctoral fellowship (FPI-UAM2012).

Appendix A. Supplementary data

Supplementary data related to this article can be found at http://dx.doi.org/10.1016/j.neuropharm.2015.02.016.

References

Bachurin, S.O., Shevtsova, E.P., Kireeva, E.G., Oxenkrug, G.F., Sablin, S.O., 2003. Mitochondria as a target for neurotoxins and neuroprotective agents. Ann. N. Y. Acad. Sci. 993, 334–344. Discussion 345–339.

Calero, O., Bullido, M.J., Clarimon, J., Hortiguela, R., Frank-Garcia, A., Martinez-Martin, P., Lleo, A., Rey, M.J., Sastre, I., Rabano, A., de Pedro-Cuesta, J., Ferrer, I.,

Calero, M., 2012. Genetic variability of the gene cluster CALHM 1-3 in sporadic Creutzfeldt-Jakob disease. Prion 6, 407–412.
Cano-Cuenca, N., Solis-Garcia del Pozo, J.E., Jordan, J., 2014. Evidence for the efficacy of latrepirdine (Dimebon) treatment for improvement of cognitive function: a meta-analysis. J. Alzheimers Dis. 38, 155–164.
Chiesi, M., Schwaller, R., Eichenberger, K., 1988. Structural dependency of the inhibitory action of benzodiazepines and related compounds on the mitochondrial Na+-Ca2+ exchanger. Biochem. Pharmacol. 37, 4399–4403.
Diaz-Prieto, N., Herrera-Peco, I., de Diego, A.M., Ruiz-Nuno, A., Gallego-Sandin, S., Lopez, M.G., Garcia, A.G., Cano-Abad, M.F., 2008. Bcl2 mitigates Ca2+ entry and mitochondrial Ca2+ overload through downregulation of L-type Ca2+ channels in PC12 cells. Cell Calcium 44, 339–352.
Dreses-Werringloer, U., Lambert, J.C., Vingtdeux, V., Zhao, H., Vais, H., Siebert, A., Jain, A., Koppel, J., Rovelet-Lecrux, A., Hannequin, D., Pasquier, F., Galimberti, D., Scarpini, E., Mann, D., Lendon, C., Campion, D., Amouyel, P., Davies, P., Foskett, J.K., Campagne, F., Marambaud, P., 2008. A polymorphism in CALHM1 influences Ca2+ homeostasis, Abeta levels, and Alzheimer's disease risk. Cell 133, 1149–1161.
Dreses-Werringloer, U., Vingtdeux, V., Zhao, H., Chandakkar, P., Davies, P., Marambaud, P., 2013. CALHM1 controls Ca2+-dependent MEK/ERK/RSK/MSK signaling in neurons. J. Cell Sci. 126, 1199–1206.
Ewing, D.F., 1974. Carbon-13-hydrogen coupling constants. III. Conformation dependence of 1J(13CH) fo r the formyl proton in aromatic aldehydes. Org. Magn. Reson. 6, 298–300.
Gallego-Sandin, S., Alonso, M.T., Garcia-Sancho, J., 2011. Calcium homoeostasis modulator 1 (CALHM1) reduces the calcium content of the endoplasmic reticulum (ER) and triggers ER stress. Biochem. J. 437, 469–475.
Giedraitis, V., Glaser, A., Sarajarvi, T., Brundin, R., Gunnarsson, M.D., Schjeide, B.M., Tanzi, R.E., Helisalmi, S., Pirttila, T., Kilander, L., Lannfelt, L., Soininen, H., Bertram, L., Ingelsson, M., Hiltunen, M., 2010. CALHM1 P86L polymorphism does not alter amyloid-beta or tau in cerebrospinal fluid. Neurosci. Lett. 469, 265–267.
Gonzalez-Lafuente, L., Egea, J., Leon, R., Martinez-Sanz, F.J., Monjas, L., Perez, C., Merino, C., Garcia-De Diego, A.M., Rodriguez-Franco, M.I., Garcia, A.G., Villarroya, M., Lopez, M.G., de Los Rios, C., 2012. Benzothiazepine CGP37157 and its Isosteric 2′-methyl analogue provide neuroprotection and block cell calcium entry. ACS Chem. Neurosci. 3, 519–529.
Inoue, K., Tanaka, N., Yamashita, F., Sawano, Y., Asada, T., Goto, Y., 2010. The P86L common allele of CALHM1 does not influence risk for Alzheimer disease in Japanese cohorts. Am. J. Med. Genet. B Neuropsychiatr. Genet. 153B, 532–535.
Koppel, J., Campagne, F., Vingtdeux, V., Dreses-Werringloer, U., Ewers, M., Rujescu, D., Hampel, H., Gordon, M.L., Christen, E., Chapuis, J., Greenwald, B.S., Davies, P., Marambaud, P., 2011. CALHM1 P86L polymorphism modulates CSF Abeta levels in cognitively healthy individuals at risk for Alzheimer's disease. Mol. Med. 17, 974–979.
Lambert, J.C., Sleegers, K., Gonzalez-Perez, A., Ingelsson, M., Beecham, G.W., Hiltunen, M., Combarros, O., Bullido, M.J., Brouwers, N., Bettens, K., Berr, C., Pasquier, F., Richard, F., Dekosky, S.T., Hannequin, D., Haines, J.L., Tognoni, G., Fievet, N., Dartigues, J.F., Tzourio, C., Engelborghs, S., Arosio, B., Coto, E., De Deyn, P., Del Zompo, M., Mateo, I., Boada, M., Antunez, C., Lopez-Arrieta, J., Epelbaum, J., Schjeide, B.M., Frank-Garcia, A., Giedraitis, V., Helisalmi, S., Porcellini, E., Pilotto, A., Forti, P., Ferri, R., Delepine, M., Zelenika, D., Lathrop, M., Scarpini, E., Siciliano, G., Solfrizzi, V., Sorbi, S., Spalletta, G., Ravaglia, G., Valdivieso, F., Vepsalainen, S., Alvarez, V., Bosco, P., Mancuso, M., Panza, F., Nacmias, B., Bossu, P., Hanon, O., Piccardi, P., Annoni, G., Mann, D., Marambaud, P., Seripa, D., Galimberti, D., Tanzi, R.E., Bertram, L., Lendon, C., Lannfelt, L., Licastro, F., Campion, D., Pericak-Vance, M.A., Soininen, H., Van Broeckhoven, C., Alperovitch, A., Ruiz, A., Kamboh, M.I., Amouyel, P., 2010. The CALHM1 P86L polymorphism is a genetic modifier of age at onset in Alzheimer's disease: a meta-analysis study. J. Alzheimers Dis. 22, 247–255.
Lermontova, N.N., Redkozubov, A.E., Shevtsova, E.F., Serkova, T.P., Kireeva, E.G., Bachurin, S.O., 2001. Dimebon and tacrine inhibit neurotoxic action of beta-amyloid in culture and block L-type Ca(2+) channels. Bull. Exp. Biol. Med. 132, 1079–1083.
Lv, R.J., He, J.S., Fu, Y.H., Shao, X.Q., Wu, L.W., Lu, Q., Jin, L.R., Liu, H., 2011. A polymorphism in CALHM1 is associated with temporal lobe epilepsy. Epilepsy Behav. 20, 681–685.
Ma, Z., Siebert, A.P., Cheung, K.H., Lee, R.J., Johnson, B., Cohen, A.S., Vingtdeux, V., Marambaud, P., Foskett, J.K., 2012. Calcium homeostasis modulator 1 (CALHM1) is the pore-forming subunit of an ion channel that mediates extracellular Ca2+ regulation of neuronal excitability. Proc. Natl. Acad. Sci. U. S. A. 109, E1963–E1971.
Mitchell, P., Moyle, J., 1967. Acid-base titration across the membrane system of rat-liver mitochondria. Catalysis by uncouplers. Biochem. J. 104, 588–600.
Moreno-Ortega, A.J., Ruiz-Nuno, A., Garcia, A.G., Cano-Abad, M.F., 2010. Mitochondria sense with different kinetics the calcium entering into HeLa cells through calcium channels CALHM1 and mutated P86L-CALHM1. Biochem. Biophys. Res. Commun. 391, 722–726.
Nicolau, S.M., de Diego, A.M., Cortes, L., Egea, J., Gonzalez, J.C., Mosquera, M., Lopez, M.G., Hernandez-Guijo, J.M., Garcia, A.G., 2009. Mitochondrial Na+/Ca2+-exchanger blocker CGP37157 protects against chromaffin cell death elicited by veratridine. J. Pharmacol. Exp. Ther. 330, 844–854.
Nicolau, S.M., Egea, J., Lopez, M.G., Garcia, A.G., 2010. Mitochondrial Na+/Ca2+ exchanger, a new target for neuroprotection in rat hippocampal slices. Biochem. Biophys. Res. Commun. 400, 140–144.
Pei, Y., Lilly, M.J., Owen, D.J., D'Souza, L.J., Tang, X.Q., Yu, J., Nazarbaghi, R., Hunter, A., Anderson, C.M., Glasco, S., Ede, N.J., James, I.W., Maitra, U., Chandrasekaran, S., Moos, W.H., Ghosh, S.S., 2003. Efficient syntheses of benzothiazepines as antagonists for the mitochondrial sodium-calcium exchanger: potential therapeutics for type II diabetes. J. Org. Chem. 68, 92–103.
Ragone, M.I., Torres, N.S., Consolini, A.E., 2013. Energetic study of cardioplegic hearts under ischaemia/reperfusion and [Ca(2+)] changes in cardiomyocytes of guinea-pig: mitochondrial role. Acta Physiol. (Oxf.) 207, 369–384.
Roosen, P.C., Kallepalli, V.A., Chattopadhyay, B., Singleton, D.A., Maleczka Jr., R.E., Smith 3rd, M.R., 2012. Outer-sphere direction in iridium C-H borylation. J. Am. Chem. Soc. 134, 11350–11353.
Tanis, J.E., Ma, Z., Krajacic, P., He, L., Foskett, J.K., Lamitina, T., 2013. CLHM-1 is a functionally conserved and conditionally toxic Ca2+-permeable ion channel in Caenorhabditis elegans. J. Neurosci. 33, 12275–12286.
Tao, Q.Q., Sun, Y.M., Liu, Z.J., Yang, P., Li, H.L., Lu, S.J., Wu, Z.Y., 2014. Lack of association between CALHM1 p.P86L variation and Alzheimer's disease in the Han Chinese population. Neurobiol. Aging 35 (1956), e1913–1954.
Taruno, A., Vingtdeux, V., Ohmoto, M., Ma, Z., Dvoryanchikov, G., Li, A., Adrien, L., Zhao, H., Leung, S., Abernethy, M., Koppel, J., Davies, P., Civan, M.M., Chaudhari, N., Matsumoto, I., Hellekant, G., Tordoff, M.G., Marambaud, P., Foskett, J.K., 2013. CALHM1 ion channel mediates purinergic neurotransmission of sweet, bitter and umami tastes. Nature 495, 223–226.
Tordoff, M.G., Ellis, H.T., Aleman, T.R., Downing, A., Marambaud, P., Foskett, J.K., Dana, R.M., McCaughey, S.A., 2014. Salty taste deficits in CALHM1 knockout mice. Chem. Senses 39, 515–528.